Positronium collisions with O_2 and CO_2

R. S. Wilde

Department of Natural Sciences, Oregon Institute of Technology, Klamath Falls, Oregon 97601, USA

H. B. Ambalampitiya and I. I. Fabrikant

Department of Physics and Astronomy, University of Nebraska, Lincoln, Nebraska 68588-0299, USA

(Dated: June 9, 2021)

Abstract

We calculate elastic and positronium (Ps) break-up cross sections for collisions of Ps with O_2 and CO_2 molecules in the fixed-nuclei approximation. We incorporate electron exchange and correlations for these processes by using the free-electron-gas model developed earlier for Ps scattering by rare-gas atoms and N_2 molecules. The results exhibit similarity between electron and Ps scattering when the cross section is plotted as a function of the projectile velocity confirming experimental observations [S. J. Brawley *et al.* Science **330**, 789 (2010)]. Below the Ps break-up threshold we observe resonance structures similar to those obtained earlier for Ps-N_2 scattering.

I. INTRODUCTION

The similarity between electron and positronium (Ps) scattering discovered ten years ago [1] continues to attract attention of experimentalists and theorists. Specifically, electron and Ps cross sections, when plotted as functions of the projectile velocity, exhibit a similar behavior and magnitude in a wide velocity range. A particularly interesting phenomenon is the recently observed resonant Ps-N_2 scattering [2] similar to resonant $e-N_2$ scattering (see [3, 4] and references therein) which was confirmed by theory [5]. Scattering by the O_2 molecule and carbon dioxide CO_2 presents a special interest in this regard. In contrast to N_2, O_2 contains two electrons in the unfilled π_g subshell. Although a low-energy Π_g resonance is observed in both $e-N_2$ and $e-O_2$ scattering, the latter resonance is extremely narrow [6, 7] and can be observed only in experiments [8, 9] with a very high energy resolution. In the case of CO_2 a sharp Π_u resonance exists in electron scattering from this molecule and there is an evidence of a resonance in Ps scattering as well [10, 11].

Note, however, that there cannot be a one-to-one correspondence between electron-molecule and Ps-molecule scattering. First, in contrast to electron-molecule scattering, in the case of Ps-molecule scattering the electron in Ps does not possess a certain projection of angular momentum on the internuclear axis, therefore the symmetry of the resonance is different in the two cases. In particular in the case of $Ps-N_2$ scattering, instead of one resonance of Π_g symmetry, we obtain three resonances of Σ_u, Π_u and Δ_g symmetries [5]. Second, the long-range parts of electron-atom/molecule interaction and Ps-atom/molecule interaction are different. In the former case it is dominated by the polarization potential decaying as the fourth power of the distance, and in the second case by the van der Waals potentials decaying as the sixth power of the distance. Therefore in the low-energy region electron and Ps scattering could exhibit different behavior.

The challenging aspect of the theoretical treatment of the Ps-atom and Ps-molecule interaction is an accurate inclusion of electron exchange and electron correlations. The exact treatment of these effects based on the close-coupling method [12–14] becomes very computationally expensive as the size of the target grows, and therefore so far this type of calculations has been carried out only for simple atomic systems like hydrogen and light rare-gas atoms. A few approximate methods for inclusion of exchange and correlation have been developed which include the pseudopotential method [15, 16], methods based on many-body

theory [17], and methods based on confined basis sets [18–21].

Recently we developed a method employing potentials based on the Free Electron Gas (FEG) model for Ps-atom or Ps-molecule scattering [22]. These potentials were used to calculate elastic scattering cross sections for Ps-N_2 [5, 23] and Ps-rare-gas-atom collisions [24]. The calculations were successful in the description of the relevant experiments, particularly in explanation of the resonance structure in the cross sections for Ps-N_2 scattering.

In what follows below we will describe our calculations of Ps$-O_2$ and Ps$-CO_2$ total scattering cross sections. As we showed in the past, the most important contribution to the total cross section for Ps scattering by a neutral target is given by elastic scattering and Ps ionization (fragmentation) or break-up. In section II we describe our FEG potentials for the Ps-O_2 and Ps-CO_2 interaction which will be used to obtain elastic scattering cross sections. In section III we describe our binary-encounter calculations of the Ps ionization cross section. In this section we also describe calculations of electron and positron scattering for these targets which are needed in the binary encounter model. We also employ FEG potentials in these calculations. In section IV we present our total cross sections for Ps scattering and in section V we briefly discuss our attempts at including orthogonality using an orthogonalizing pseudopotential (OPP). Section VI is a brief conclusion. As it has become customary since the discovery of similarity between electron and Ps scattering [1], we plot all cross sections as functions of the projectile velocity. Atomic units are used throughout unless stated otherwise.

II. PS SCATTERING POTENTIALS

For elastic Ps-O_2 and Ps-CO_2 scattering we determine the scattering potentials in the same way as was done for Ps-N_2 scattering [5]. In ref. [22] we have derived expressions for the exchange and correlation energies as functions of the Fermi energy. In order to introduce the dependence of these energies on the projectile position relative to the target we determine the Fermi energy in terms of the charge density of the O_2 or CO_2 ground state. The Ps-molecule scattering potentials obtained in this way are then expanded in Legendre polynomials. In all of our scattering calculations the static potential and all FEG potentials depend on the ground state electronic charge density The charge density for O_2 was obtained by performing the Restricted Hartree-Fock (RHF) calculations [25] implemented in the GAUSSIAN 03W

suite of programs [26]. The 6-31G* basis set [25] was employed for the RHF geometry optimization of the O_2 molecule. The charge density for CO_2 was determined from the molecular orbitals of Yoshimine and McLean [27]

The correlation potential at large distances is matched to the van der Waals potential with a cut-off of the form

$$V_W(\mathbf{R}) = -\frac{C_0 + C_2 P_2(\cos\chi)}{(R^2 + R_c^2)^3} \tag{1}$$

where R is the position of the center of Ps relative to the center of mass of the molecule. χ is the angle between $\mathbf{R}$ and the internuclear axis, and R_c is a cutoff radius. The van der Waals coefficients C_0 and C_2 were calculated from the London formula using the molecular and Ps polarizabilities.

For O_2 we use the polarizabilities α_0=10.6 a.u. and α_2=4.77 a.u. giving $C_0 = 91.5$ a.u. and $C_2 = 41.2$ a.u. In order for the correlation potential to match smoothly to the asymptotic form we have chosen a cutoff radius of $R_c = 1.19$ a.u. and for the spherical component $\lambda = 0$ switched from the correlation potential to the asymptotic form at R=3.4 a.u.

For CO_2 we use the polarizabilities α_0=17.76 a.u. and α_2=9.49 a.u. giving $C_0 = 160.5$ a.u. and $C_2 = 85.8$ a.u. In order for the correlation potential to match smoothly to the asymptotic form we have chosen a cutoff radius of $R_c = 0.3$ a.u. and for the spherical component $\lambda = 0$ switched from the correlation potential to the asymptotic form at R=4.58 a.u.

In Fig. 1 we show the lowest two components (λ=0,2) of the Legendre expansion for the total potential (exchange plus correlation) for a Ps velocity of 0.01 a.u. and compare them with the potentials for Ps-N_2 scattering [5]. The potentials for O_2 and N_2 are very similar, but the Ps-O_2 potential is more attractive for intermediate values of R. For Ps-CO_2 the λ=0 component is much more attractive near R=0 due to the presence of the carbon atom at the origin. The potential for CO_2 is generally more attractive than for O_2 and N_2 at larger values of R, partly due to the stronger van der Waals interaction for CO_2, but mostly due to the larger internuclear separation.

We solve the Schrödinger equation with these potentials using the integral equation method of [28] to obtain elastic Ps scattering cross sections. These elastic cross sections will be presented in section IV along with our total cross sections.

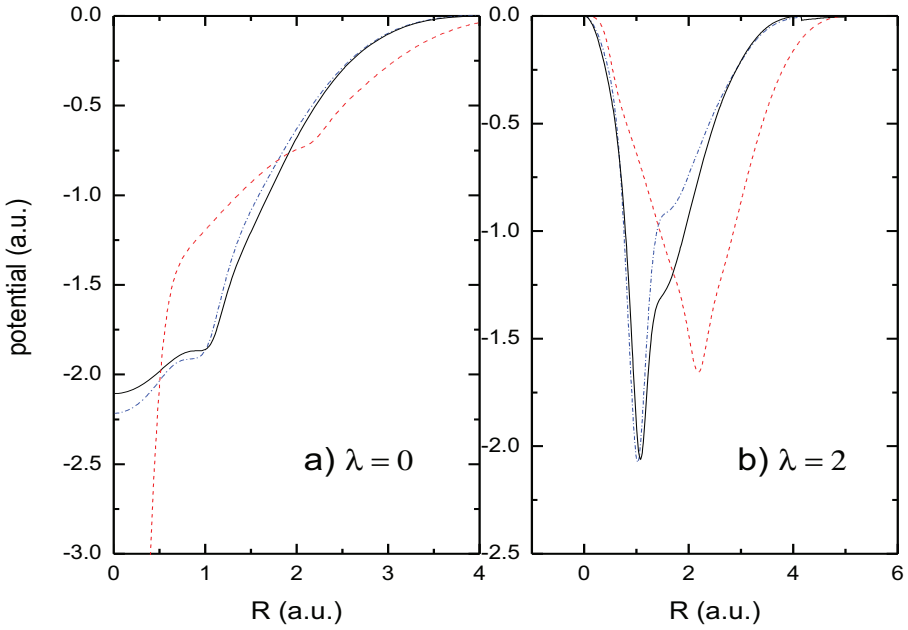

FIG. 1. First two Legendre components (λ=0,2) of the total FEG potentials (exchange plus correlation) for Ps-O_2: solid lines, for Ps-CO_2: red dashed lines and for Ps-N_2: blue dash-dot lines.

III. IONIZATION

Apart from elastic scattering, the largest contribution to the total cross section for positronium collisions is expected to be Ps ionization (fragmentation) or break-up. In the present paper we employ the binary encounter approximation to calculate cross sections for Ps ionization [29, 30]. We have previously applied this approximation to calculate Ps ionization cross sections in collision with rare gas atoms Ar, Kr and Xe [16] which were in good agreement with previous calculations using the impulse approximation [31]. The binary encounter approximation for Ps ionization was extended to non-spherical interactions and applied to Ps-N_2 scattering in [5].

The ionization amplitude in the binary encounter approximation is expressed through the body frame T-matrix elements in the fixed nuclei approximation for electron and positron scattering by the target. To calculate the scattering matrices we have solved the Schrödinger equation for electron and positron scattering using the integral equation method [28] in the

static-exchange plus polarization approximation [32] using the potentials described below. We emphasize that, in this section, our goal is to obtain scattering matrices for electron and positron scattering that produce cross sections in as good agreement with experimental data as possible using potentials that do not use any adjustable parameters. These scattering matrices then serve as input in the binary encounter approach that allows us to calculate Ps ionization cross sections. For comparative purposes we have also tried using a semi-empirical correlation/polarization potential for e^+-O_2 scattering.

For e^--O_2 elastic scattering the static potential is attractive. We also use the Hara free electron gas approximation (HFEGE) for the exchange potential [33]. For the correlation-polarization potential we use the FEG model of O'Connell and Lane [34] which was successfully applied by them to electron scattering by rare-gas atoms. To our knowledge, this is the first time this model of correlation has been applied to electron molecule-collisions. In this model the long-range polarizability is enforced by switching to the long range form at the distance at which it intersects with the FEG correlation potential.

In Fig. 2 panel (a) we show our calculated elastic e^--O_2 cross sections compared with the recommended elastic cross sections of Itikawa [35] and the measurements of Murphy [36] which extend to very low velocities. The agreement between our calculated cross sections and the measurements of Murphy [36] at low velocities is very good. At higher velocities the present calculations are slightly smaller than the experimental values, but overall the agreement is good. At low velocities our cross section disagrees with the R-matrix results of Higgins *et al.* [7] which does not exhibit a strong downturn towards lower energies (velocities) observed in our calculations and confirmed by Murphy's measurements [36]. As explained in [7] this is probably due to the omission of long-range polarization effects in the expansion of the scattering wavefunction in the R-matrix calculation. We also do not detect a very narrow Π_g resonance obtained in the R-matrix calculations at E = 0.0554 Ryd (velocity 0.235 a.u.). We note that the structure in the experimental data due to the Π_g resonance is prominent in the vibrational excitation data, but not as much in elastic scattering [35]. Lastly, as shown in the R-matrix calculations of Higgins et al. [7] the resonance structure is very sensitive to the internuclear separation. When we use only the static potential for e^--O_2 elastic scattering we do observe a Π_g resonance structure, but when we add exchange and correlation it disappears. It could be possible that our model potential is too attractive, and the resonance position is shifted towards lower energies, where it becomes even narrower,

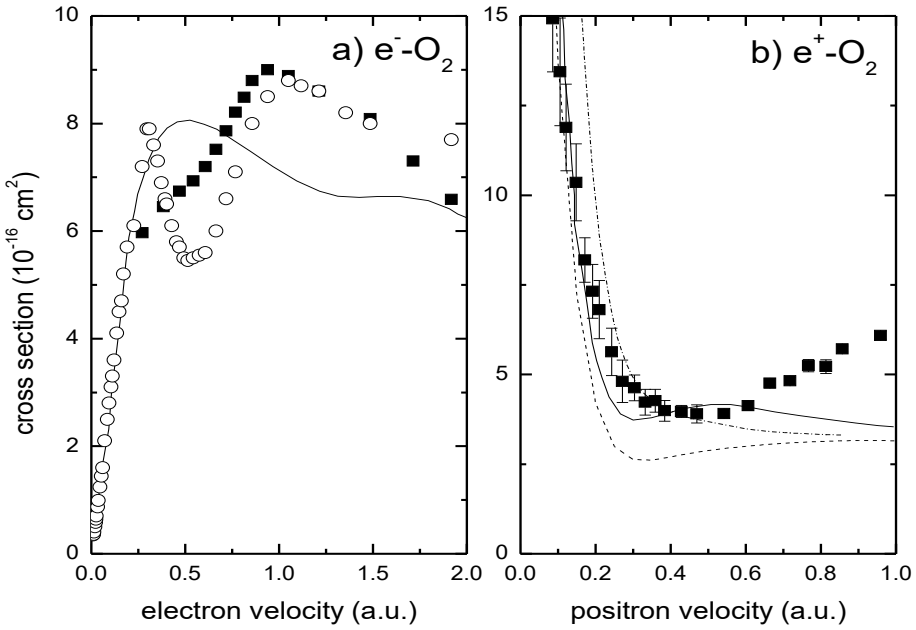

FIG. 2. a) Elastic e^-−O_2 cross sections as functions of electron velocity. Solid line: present calculation. Squares: recommended elastic cross sections of Itikawa [35]; circles: elastic cross sections compiled by Murphy [36]. b) Total elastic e^+−O_2 cross section as a function of positron velocity. Solid line: present calculation including Σ, Π and Δ symmetries and using semi-empirical polarization of Eq. 2. Dashed line: present calculations using correlation potential of O'Connell and Lane [34]. Dot-dashed line: calculations of Tenfen *et al.* [37]. Squares: measured total cross sections of Chiari *et al.* [38].

or even towards negative energies, however, we believe that the general agreement of our results with experimental measurements should provide a good estimate of the Ps ionization cross section.

For positron scattering the static potential is repulsive instead of attractive. We can add to it a semi-empirical polarization potential of the form

$$V_{pol}(r) = \left[-\frac{\alpha_0}{2r^4} - \frac{\alpha_2}{2r^4} P_2(\cos\theta)\right] C(r) \tag{2}$$

where

$$C(r) = 1 - \exp[-(r/r_c)^p]. \tag{3}$$

is a cutoff function and r_c is an adjustable cutoff parameter. For the polarization potential we use $\alpha_0 = 10.6$ a.u. and $\alpha_2 = 4.77$ a.u which are also the values used in the recent e^+-O_2 calculations of Tenfen *et al.* [37]. In order to get good agreement with the experimental values of Chiari *et al.* [38] we use p=1, but have had to choose different values of r_c depending on the scattering symmetry. For gerade symmetries ($\Sigma_g, \Pi_g, \Delta_g$) we have used $r_c = 2.3$ a.u. and for ungerade symmetries ($\Sigma_u, \Pi_u, \Delta_u$) we have used $r_c = 1.29$ a.u. We show our calculated total elastic e^+-O_2 cross section in Fig. 2 panel (b) and compare it with the experimental results of Chiari *et al.* [38] and the calculations of Tenfen *et al.* [37].

It is often quite difficult to obtain a good fit to the experimental cross section for positron scattering by varying the parameters of the semi-empirical potential and we haven't been able to obtain a good fit for all velocities up to the Ps formation threshold for e^+-CO_2 scattering. Therefore, we have tried using the correlation/polarization potential of ref. [34] for positron scattering by both molecular targets as well. We show the resulting elastic cross section in this case for e^+-O_2 scattering in Fig. 2 (b).

In Fig. 3 (a) we show our results for the e^-CO_2 total elastic scattering cross section using the HFEGE exchange potential and the FEG correlation potential of O'Connell and Lane [34]. Our cross sections are generally a little larger than the recommended values [39] and the calculations of Morrison *et al.* [40] We emphasize, however, that those calculations employed the semi-empirical polarization potential, whereas our calculations, which use the correlation potential of [34], do not employ an adjustable cutoff parameter. Also the calculations of [40] include only Σ and Π scattering symmetries whereas ours include Δ symmetries as well. The sharp rise of the cross section at low velocities and the position of the Π_u resonance that has also been seen in other theoretical studies [40–42] is well reproduced by this model.

In Fig. 3 (b) we show our results for e^+-CO_2 scattering As mentioned above, we could not find a set of parameters for Eq. (2) that gave good agreement with the measurements of Zecca *et al.* [43] or of Hoffman *et al.* [44] over the entire velocity range, therefore we have used only the correlation model of O'Connell and Lane [34] here. As for O_2 this model of correlation gives e^+-CO_2 cross sections that are slightly smaller than the experimental values. Other calculations agree better with experiment at intermediate energies (velocities) [45–47] As an example we show the body-frame vibrational close-coupling calculations (BF-VCC) calculations of Gianturco and Mukherjee [46] in Fig. 3 (b). As discussed by Morrison

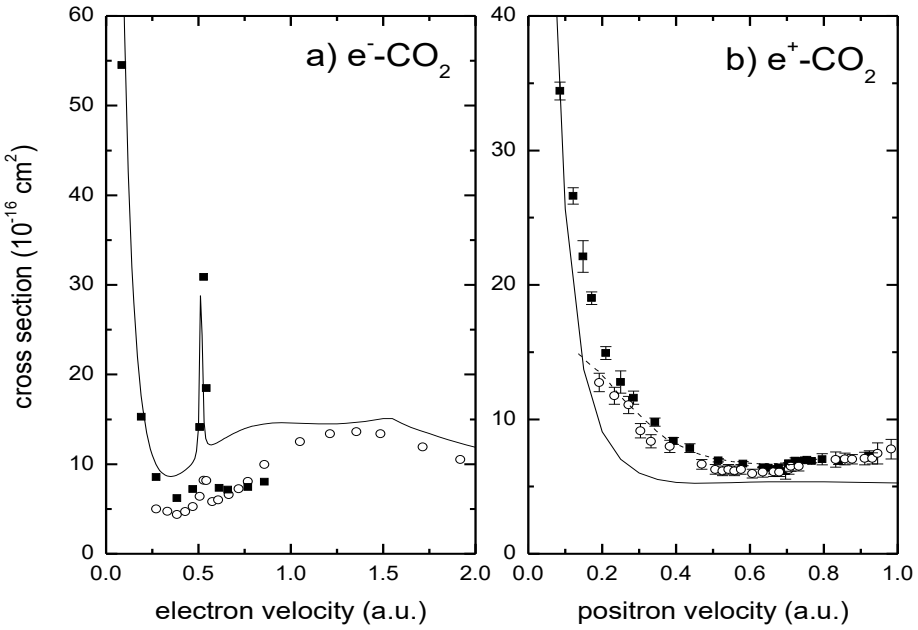

FIG. 3. a) Elastic e^--CO_2 cross sections as functions of electron velocity. Solid line: present calculation. Circles: recommended elastic cross sections of Itikawa [39]; squares: elastic cross sections calculated by Morrison *et al.* [40]. b) Total elastic e^+-CO_2 cross section as a function of positron velocity. Solid line: present calculation including Σ, Π and Δ symmetries and using FEG correlation potential of [34]. Squares: measured total cross sections of Zecca *et al.* [43]; circles: measured cross sections of Hoffman *et al.* [44]. Dashed line: BF-VCC calculations of [46].

et al. [48], for the case of e^+-H_2 scattering, the polarization potential for positrons should be more attractive at intermediate distances than for electrons due to the attraction between the positron and the electron cloud of the target molecule. By using the same correlation-polarization potential as for electron scattering we are neglecting this effect and its inclusion in the FEG model of correlation for positron scattering might improve the agreement with experiment. On the other hand our calculations agree well with the sharp rise in the experimental data for low velocities and again we feel that they should provide a good estimate of the Ps-CO_2 ionization cross section.

Using the T-matrices corresponding to the above described elastic scattering calculations we have used the binary encounter method [5] to calculate the Ps ionization cross sections.

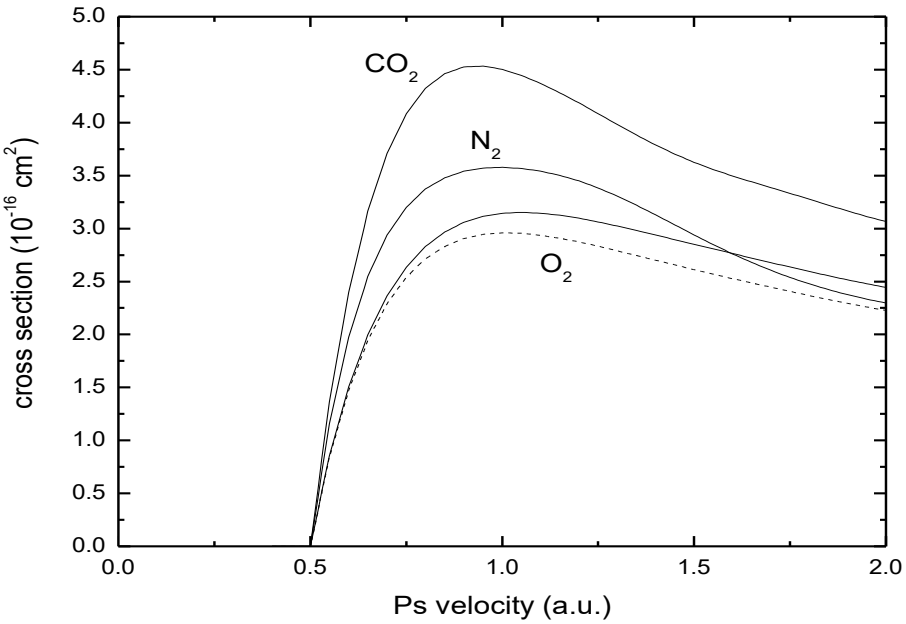

FIG. 4. Ps ionization (fragmentation) cross sections calculated using the binary encounter approximation for Ps-CO_2, Ps-N_2 and Ps-O_2, in order of decreasing magnitude at a Ps velocity of 1 a.u. Solid lines are calculated using the FEG correlation potential of [34] for both the electron and positron contribution. The dashed line represents the Ps-O_2 ionization cross section using the semi-empirical correlation potential of Eq. 2 for the positron contribution.

In Fig. 4 we show our Ps-O_2 and Ps-CO_2 binary-encounter ionization cross sections and compare them with our previous calculations for N_2. For CO_2 we use the FEG correlation potential of [34] in the calculation of the positron contribution while for O_2 we present results employing both the FEG correlation potential and semi-empirical potential of Eq. (2).

We see that the CO_2 cross section is largest and O_2 is smallest. Generally, this mirrors the overall size of the cross sections for electron and positron scattering by these molecules. We note, however, that for O_2 the ionization cross section is slightly smaller if we use Eq. (2) in the calculation of the positron contribution. This is despite the e^+-O_2 cross section being larger in this case and shows that there is not an entirely direct correlation between the size of the elastic electron and positron cross sections and the Ps ionization cross section. The ionization cross section is directly related to the differential cross section for electron

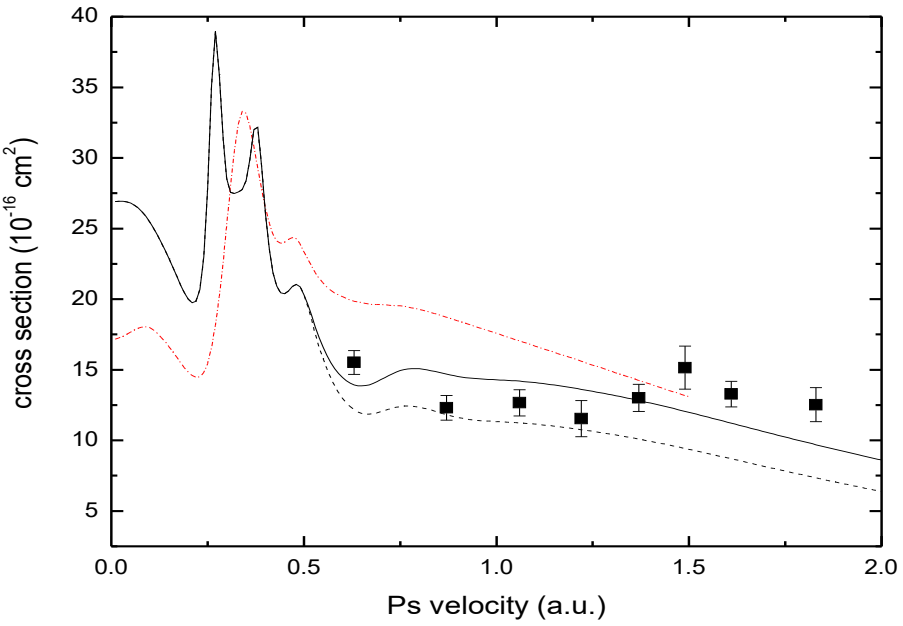

FIG. 5. Cross sections for Ps scattering with O_2. Solid line: theory, total cross section; dashed line: theory, elastic cross section. Squares: measurements of Brawley *et al.* [1]. For comparison the dash-dot red line is the total Ps-N_2 cross section of [5].

and positron scattering, not to the total elastic cross section.

IV. ELASTIC AND TOTAL CROSS SECTIONS

In Fig. 5 we present the calculated elastic and total cross sections for Ps-O_2 scattering. At higher velocities the total cross section (elastic plus ionization) agrees quite well with experiment. At low velocities, below the Ps-ionization threshold (v=0.5 a.u.) the calculated cross sections exhibit resonance structures. These resonances are similar to those seen for Ps-N_2 scattering [5] except they are shifted to slightly lower velocities and are slightly narrower. This might not be unexpected since, as we can see from Fig. 1 the Ps-O_2 potentials are generally more attractive than the Ps-N_2 potentials, particularly for intermediate values of R.

In Fig. 6 we show the partial cross sections for all Ps-O_2 scattering symmetries included

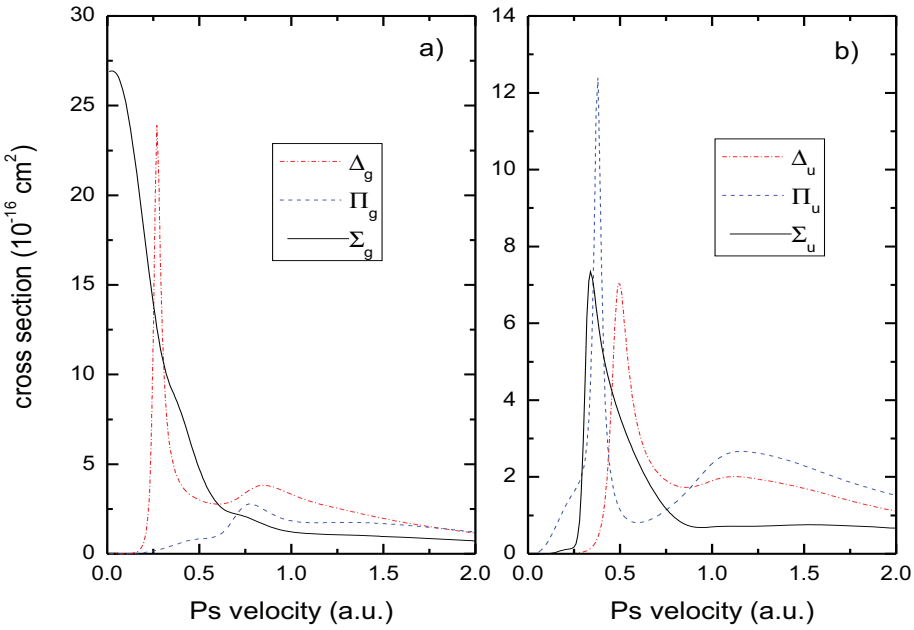

FIG. 6. Partial cross sections for Ps-O_2 elastic scattering a) even (gerade) scattering symmetries. b) odd (ungerade) scattering symmetries.

in the present elastic cross sections. We see that the sharp resonance peaks are mainly due to resonances in the Δ_g, Π_u symmetries, but there are also resonances in the Σ_u and Δ_u symmetries. We have seen previously similar features in all of these symmetries for Ps-N_2 scattering when using the FEG potentials, see Fig. 7 of ref. [5]. These resonances are just 'pulled' to lower velocities by the more attractive Ps-O_2 interaction.

In Fig. 7 we present the calculated elastic and total cross sections for Ps-CO_2 scattering. The results are similar to those obtained for Ps-O_2 scattering. Again we see good agreement with experiment above the Ps-ionization threshold. There is some indication of a resonance at $v = 0.6$ a.u. in the experimental data, but overall the theoretical resonance structure is more pronounced than in measured results for both CO_2 and N_2. In Fig. 8 we show the partial cross sections for Ps-CO_2 scattering. Once again we see similar resonance structures as for O_2. In Fig. 9 we compare our total Ps cross section with experiment and recommended values of the total e^-−O_2 and e^-−CO_2 scattering cross sections. We see that above the Ps ionization threshold the electron and Ps cross sections become similar which confirms the

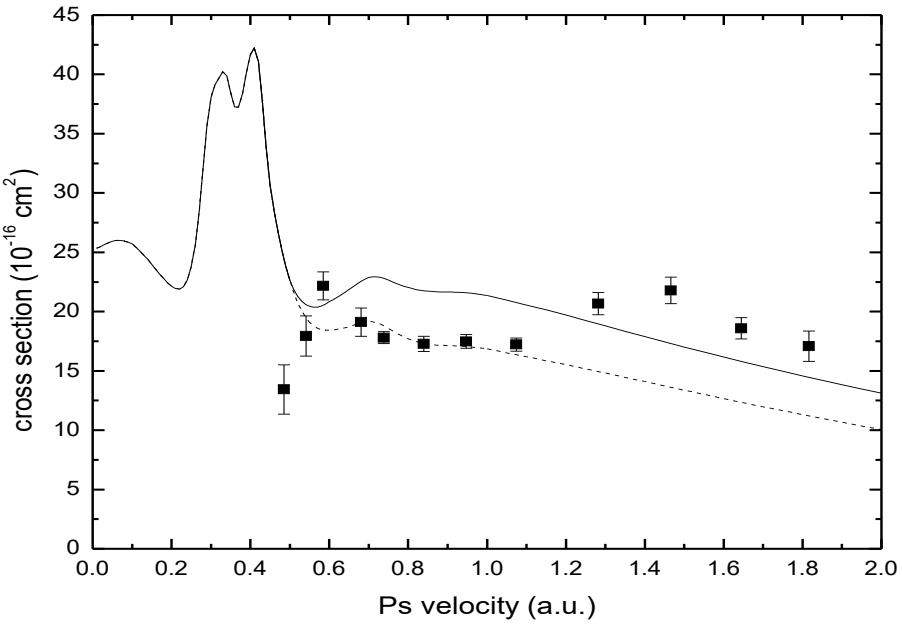

FIG. 7. Cross sections for Ps scattering with CO_2. Solid line: theory, total cross section; dashed line: theory, elastic cross section. Squares: measurements of Brawley *et al.* [10].

experimental observations. Below the threshold the electron and Ps cross sections are quite different. This might not be unexpected since the long-range correlation is quite different in the two cases.

V. ORTHOGONALITY

In electron-atom and electron-molecule scattering use of the static-exchange approximation leads to overlap terms between the target orbitals and the scattering wavefunction [32]. These terms are due to the anti-symmetric character of the total many-electron wavefunction. When the static-exchange equations are solved exactly using the full non-local exchange kernel the scattering wave-function is ensured to be orthogonal to the occupied target orbitals for closed shell targets [49, 50]. When local approximations to the exchange potential are made orthogonality is no longer ensured. The effect of including orthogonality in the local calculations have been studied for electrons by rare-gas atoms using a Lagrange

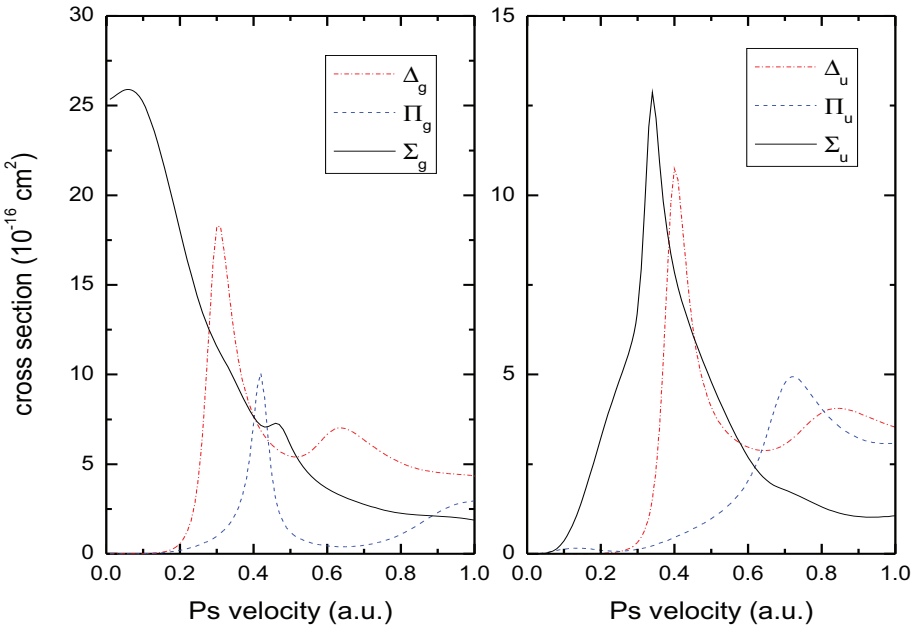

FIG. 8. Partial cross sections for Ps-CO_2 elastic scattering a) even (gerade) scattering symmetries. b) odd (ungerade) scattering symmetries.

multiplier technique [34] and was found to be small.

To incorporate orthogonality in electron and Ps scattering calculations the Orthogonalizing Pseudopotential (OPP) method has been suggested [51, 52]. In this method a non-local repulsive potential containing a strength parameter γ is added to the electron-molecule Hamiltonian. The strength parameter is made large enough so that orthogonality is enforced and the scattering calculations are converged in the sense that further increase of γ leads to a negligible change in the phase shifts and cross sections.

Our application of this method to Ps scattering by rare gas atoms [24] turned out to be successful, but all attempts to add OPP to Ps interaction with molecules led to Hamiltonians which appear to be too repulsive to describe resonances in these systems. This is illustrated for Ps-N_2 collisions in Fig. 10. We see here that inclusion of the OPP removes all resonance structure. Furthermore, we encounter severe numerical difficulties which affects convergence when iterative methods are used to solve the coupled integro-differential equations especially as the strength parameter is increased.

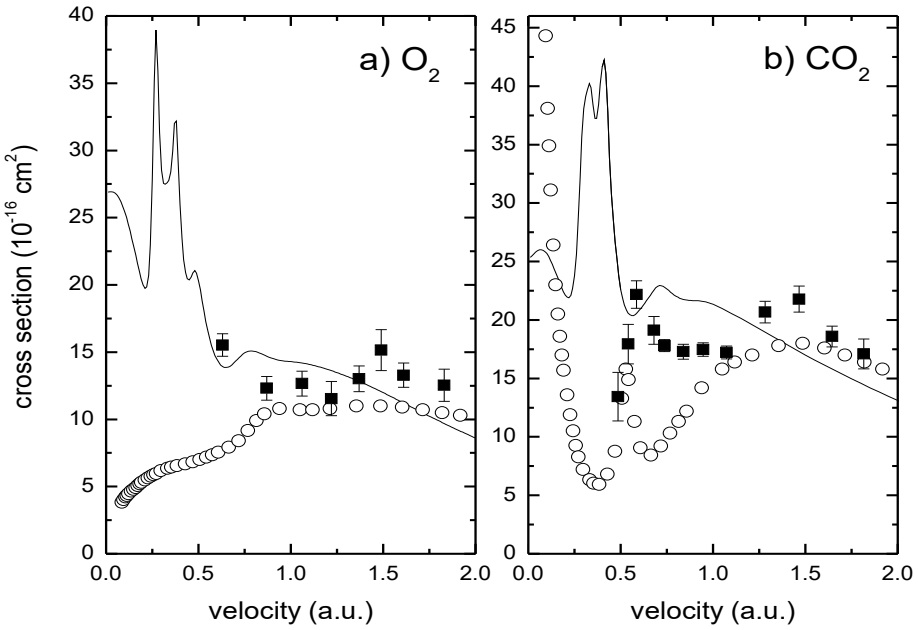

FIG. 9. Total scattering cross sections for Ps and e^- scattering by a) O_2 and b) CO_2. Solid lines: present results; Squares: Ps experiment, O_2 [1] and CO_2 [10]; Circles: recommended e^- total scattering cross sections for O_2 [35] and CO_2 [39].

In this connection we note that Mitroy *et al.* [51, 52] has made the following observations regarding the OPP method:

1. In their one state calculation [52] of Ps-He scattering the phase shift showed no sign of stabilizing as the strength parameter γ was increased. They concluded that a Ps-basis with only one scattering state does not have the flexibility to give a zero overlap with the 1s core orbital. A previous investigation of the application of the OPP to bound state problems also revealed that the quality of the basis did have an impact on the ability of the calculation to achieve a zero overlap and this could have an impact upon the computed energy and rate for positron annihilation [51].

2. The use of excessively large γ degrades the quality of the wave function as it attempts to satisfy a condition that is increasingly difficult to fulfill with a finite basis.

3. The OPP operator is best used in situations where it is feasible to use a sufficiently large channel space so that the expectation value of the OPP operator can be sufficiently

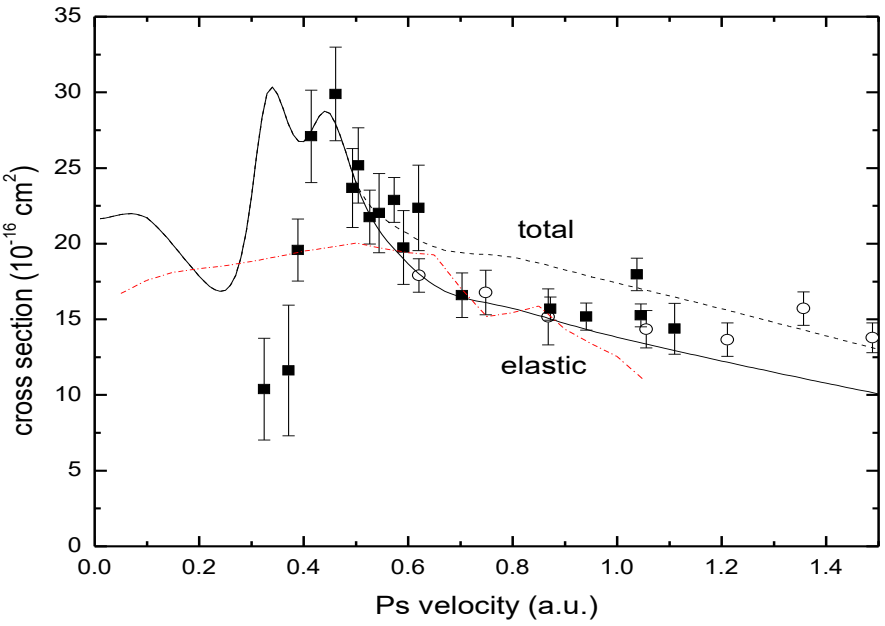

FIG. 10. Cross sections for Ps scattering with N_2. Solid line: theory, total cross section; dashed line: elastic cross section obtained by using FEG potentials [5]; red dash-dot line: elastic cross section including OPP, Squares: experiment, Brawley *et al.* [1]; open circles: Shipman *et al.* [2].

close to zero.

We have also attempted to employ the OPP method to electron-molecule scattering and show our results in Fig. 11 for e^-−H_2 elastic scattering, including only FEG potentials as well as including the OPP. In this case we see once again that the FEG potentials by themselves give good agreement with experiment, while inclusion of the OPP destroys this agreement at low velocities.

To conclude, the OPP can sensibly be applied to the scattering of two composite objects, but it is important to ensure that the wave function is sufficiently flexible so that the expectation of the OPP operator can be made sufficiently small and therefore does not influence the phase shifts in a manner other than reason for which it was originally introduced. We have found that these requirements are not satisfied in e^-−M and Ps-M problems with the exchange and correlation potentials we are employing, therefore the OPP method has not been used further in the present calculations.

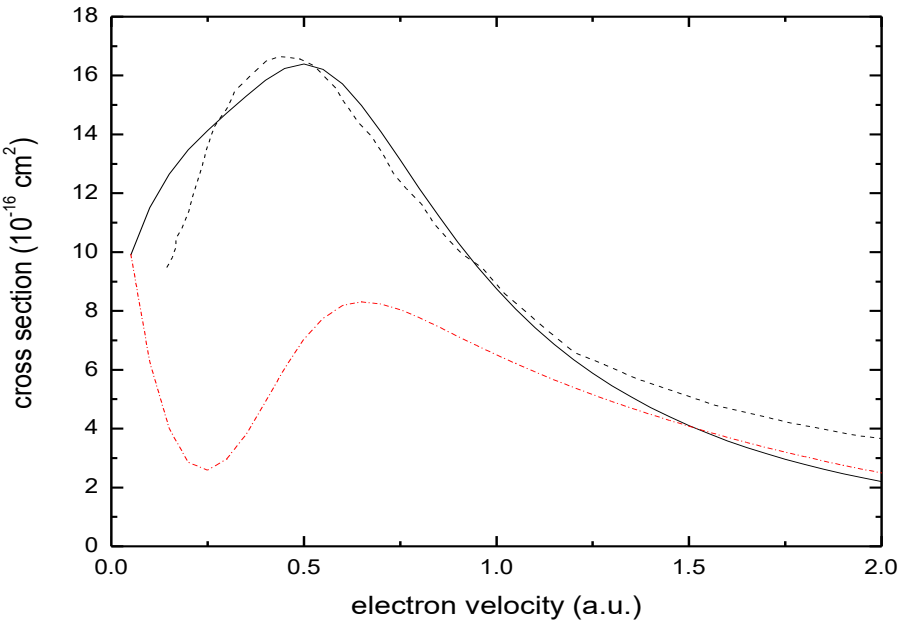

FIG. 11. Cross sections for electron scattering with H_2. Solid line, present elastic cross section using FEG potentials; red dash-dot line, present elastic cross section including OPP; dashed line, total cross section of Kauppila and Stein [53]

VI. CONCLUSION

We have studied the application of local Free Electron Gas (FEG) potentials to electron, positron and Ps scattering by O_2 and CO_2. In general the agreement with experiment is good in all cases, including for O_2 which is an open shell target.

For Ps scattering our total cross sections, including elastic scattering and ionization, agree well with experiment for velocities above the ionization threshold. Below the threshold our calculations show a rich resonance structure. Similar resonances have been observed experimentally near the threshold for N_2 and CO_2. However, it appears that our cross sections below the threshold are quite larger than the experimental values. This implies that more theoretical and experimental study is needed in this region.

We have also attempted to include orthogonality effects using an Orthogonalizing Pseudopotential (OPP) and found that this is not entirely appropriate for e^-−M or Ps-M scat-

tering. It might be possible to generalize the Lagrange multiplier method of including orthogonality to Ps collisions in order to further study these effects.

ACKNOWLEDGMENTS

The authors are grateful to G. Laricchia for stimulating discussions. This work was supported by the National Science Foundation under Grant Nos. PHY-1803744 and PHY-2011262 and was completed utilizing the Holland Computing Center of the University of Nebraska, which receives support from the Nebraska Research Initiative.

---

[1] S. J. Brawley, S. Armitage, J. Beale, D. E. Leslie, A. I. Williams, and G. Laricchia, Science **330**, 789 (2010).

[2] M. Shipman, S. J. Brawley, L. Sarkadi, and G. Laricchia, Phys. Rev. A **95**, 032704 (2017).

[3] B. I. Schneider, Phys. Rev. A **24**, 1 (1981).

[4] W. Sun, M. A. Morrison, W. A. Isaacs, W. K. Trail, D. T. Alle, R. J. Gulley, M. J. Brennan, and S. J. Buckman, Phys. Rev. A **52**, 1229 (1995).

[5] R. S. Wilde and I. I. Fabrikant, Phys. Rev. A **97**, 052708 (2018).

[6] C. J. Noble and P. G. Burke, Phys. Rev. Lett. **68**, 2011 (1992).

[7] K. Higgins, C. J. Noble and P. G. Burke, J. Phys. B **27**, 3203 (1994).

[8] J. E. Land and W. Raith, Phys. Rev. A **9**, 1592 (1974).

[9] M. Allan, J. Phys. B: At. Mol. Opt. Phys. **28**, 5163 (1995).

[10] S. J. Brawley, A. I. Williams, M. Shipman and G. Laricchia, Phys. Rev. Lett. **105**, 263401 (2010).

[11] M. Shipman, S. J. Brawley, L. Sarkadi and G. Laricchia, Phys. Rev. A **95**, 032704 (2017).

[12] M. T. McAlinden, F. G. R. S. MacDonald, and H. R. J. Walters, Can. J. Phys. **74**, 434 (1996).

[13] J. E. Blackwood, C. P. Campbell, M. T. McAlinden and H. R. J. Walters, Phys. Rev. A **60**, 4454 (1999).

[14] J. E. Blackwood, M. T. McAlinden, and H. R. J. Walters, J. Phys. B **35**, 2661 (2002).

[15] I. I. Fabrikant and G. F. Gribakin, Phys. Rev. A **90**, 052717 (2014).

[16] G. F. Gribakin, A. R. Swann, R. S. Wilde, and I. I. Fabrikant, J. Phys. B **49**, 064004 (2016).

[17] D. G. Green, A. R. Swann, and G. F. Gribakin, Phys. Rev. Lett. **120**, 183402 (2018).

[18] J. Mitroy and I. A. Ivanov, Phys. Rev. A **65**, 012509 (2001).

[19] J. Mitroy and M. W. J. Bromley, Phys. Rev. A **67**, 034502 (2003).

[20] A. R. Swann and G. F. Gribakin, Phys. Rev. A **97**, 012706 (2018).

[21] J.-Y. Zhang, M.-S. Wu, Y. Qian, X. Gao, Y.-J. Yang, K. Varga, Z.-C. Yan and U. Schwingenschlögl, Phys. Rev. A **100**, 032701 (2019).

[22] I. I. Fabrikant and R. S. Wilde, Phys. Rev. A **97**, 052707 (2018).

[23] R. S. Wilde and I. I. Fabrikant, J. Phys. B **53**, 185202 (2020).

[24] R. S. Wilde and I. I. Fabrikant, Phys. Rev. A **98**, 042703 (2018)

[25] W. J. Hehre, L. Radom, P. v. R. Schleyer and J. A. Pople, *Ab initio Molecular Orbital Theory* (John Wiley and Sons Inc., New York, 1986).

[26] M. J. Frisch *et al.*, Revision B.02 GAUSSIAN 03, (Gaussian Inc., Wallingford, CT, 2003).

[27] M. Yoshimine and A. D. McLean, Int. J. Quantum Chem. **1S**, 313 (1967); A. D. McLean and M. Yoshimine, IBM J. Res. Dev. **12**, 206 (1968).

[28] M. A. Morrison, in *Electron-Molecule and Photon-Molecule Collisions*, eds. T. Rescigno, V. McKoy and B. Schneider (Plenum Press, New York 1979), p. 15.

[29] B. M. Smirnov, in *The Physics of Electronic and Atomic Collisions*, eds. J. S. Risley and R. Geballe (University of Washington Press, Seattle, 1976), p. 701.

[30] M. R. Flannery, in *Rydberg States of Atoms and Molecules*, eds. R. F. Stebbings and F. B. Dunning (Cambridge University Press, Cambridge 1983), p. 393.

[31] C. Starrett, M. T. McAlinden, and H. R. J. Walters, Phys. Rev. A **72**, 012508 (2005).

[32] N. F. Lane, Rev. Mod. Phys. **52**, 29 (1980).

[33] S. Hara, J. Phys. Soc. Japan **22**, 710 (1967).

[34] J. K. O'Connell and N. F. Lane, Phys. Rev. A **27**, 1893 (1983).

[35] Y. Itikawa, J. Phys. Chem. Ref. Data **38**, 1 (2009).

[36] T. Murphy, *Total and differential electron collision cross sections for O_2 and N_2*, Rep. LA-11288-MS, Los Alamos Natl. Lab., Los Alamos, N. M. (1988), Table 2.

[37] W. Tenfen, M. Barp and F. Arretche, Phys. Rev. A **99**, 022703 (2019).

[38] L. Chiari, A. Zecca, S. Girardi, E. Trainotti,G Garcıa, F. Blanco5, R. P. McEachran and M. J. Brunger, J. Phys. B. At. Mol. Opt. Phys. **45**, 215206 (2012).

[39] Y. Itikawa, J. Phys. Chem. Ref. Data **31**, 749 (2002).

[40] M. A. Morrison, N. F. Lane and L. A. Collins, Phys. Rev. A **15** 2186 (1977).

[41] M.G. Lynch, D. Dill, J. Siegel, J. L. Dehmer, J. Chem. Phys. **71**, 4249 (1979).

[42] D. Thirumalai, K. Onda, D. G. Truhlar, J. Chem. Phys. **74**, 6792 (1981).

[43] A. Zecca, C. Perazzolli, N Moser, D Sanyal, M. Chakrabarti, and M. J. Brunger, Phys. Rev. A **74** 012707 (2006).

[44] K. R. Hoffman, M. S. Dababneh, Y.-F. Hsieh, W. E. Kauppila, V. Pol, J. H. Smart, and T. S. Stein, Phys. Rev. A **25**, 1393 (1982).

[45] F. A. Gianturco and P. Paioletti, Phys. Rev. A 55, 3491 (1997).

[46] F. A. Gianturco and T. Mukherjee, J. Phys. B 30, 3567 (1997).

[47] M. Horbatsch and J. W. Darewych, J. Phys. B 16, 4059 (1983).

[48] M. A. Morrison, T. L. Gibson and D. Austin, J. Phys. B: At. Mol. Phys.**17** 2725 (1984).

[49] M. J. Seaton, Comments At. Mol. Phys. 1, 184 (1970).

[50] M. A. Morrison and L. A. Collins, Phys. Rev. A **23**, 127 (1981).

[51] J. Mitroy and G. G. Ryzhikh, Comput. Phys. Commun. **123**, 103 (1999).

[52] I. A. Ivanov, M. W. J. Bromley, and J. Mitroy, Comput. Phys. Commun. **152**, 9 (2003).

[53] W. E. Kauppila and T. S. Stein, Adv. At. Mol. Opt. Phys. **26**, 1 (1989)